

NJC

Accepted Manuscript



This article can be cited before page numbers have been issued, to do this please use: H. Wen, J. Ma, J. Chen, Z. Ke, D. Zou and Q. Li, *New J. Chem.*, 2019, DOI: 10.1039/C9NJ01331H.



This is an Accepted Manuscript, which has been through the Royal Society of Chemistry peer review process and has been accepted for publication.

Accepted Manuscripts are published online shortly after acceptance, before technical editing, formatting and proof reading. Using this free service, authors can make their results available to the community, in citable form, before we publish the edited article. We will replace this Accepted Manuscript with the edited and formatted Advance Article as soon as it is available.

You can find more information about Accepted Manuscripts in the [author guidelines](#).

Please note that technical editing may introduce minor changes to the text and/or graphics, which may alter content. The journal's standard [Terms & Conditions](#) and the ethical guidelines, outlined in our [author and reviewer resource centre](#), still apply. In no event shall the Royal Society of Chemistry be held responsible for any errors or omissions in this Accepted Manuscript or any consequences arising from the use of any information it contains.

Heavy atom free 1,1,4,4-tetraphenylbuta-1,3-diene with aggregation induced emission for photodynamic cancer therapy

Huijuan Wen^a, Juan Ma^a, Jianjiao Chen^b, Zhen Ke^b, Dengfeng Zou^{*b}, Qiaoyun Li^{*c}

Received 00th January 2018,
Accepted 00th January 2018

DOI: 10.1039/x0xx00000x
www.rsc.org/

Common organic molecules usually suffer from aggregation caused quenching (ACQ), which is disadvantageous for imaging guided phototherapy. It is of tremendous significance for a photosensitizer to be well soluble and simultaneously remain highly fluorescent in aqueous solution. Heavy atom free 1,1,4,4-tetraphenylbuta-1,3-diene (denoted as **TPD**) with aggregation induced emission (AIE) was designed and synthesized by Knoevenagel reaction. 1,2-distearoyl-sn-glycero-3-phospho-ethanolamine-*N*-[methoxy(polyethyleneglycol)-₂₀₀₀] (DSPE-PEG-₂₀₀₀) coated **TPD** nanoparticles (NPs) show high singlet oxygen generation ability with singlet oxygen sensor green (SOSG) as a probe and still remain highly fluorescent in aqueous solution. *In vitro* cytotoxicity assay demonstrates that these NPs have a half-maximal inhibitory concentration (IC₅₀) as low as 8.2 μg/mL. Meanwhile, *in vivo* fluorescence imaging shows that these NPs can passively target to the tumor by the enhanced penetration and retention (EPR) effect within 6 h. Furthermore, *in vivo* phototherapy suggests that **TPD** NPs are able to inhibit the growth of tumor after irradiation without side effects to the normal tissues, including heart, liver, spleen, lung and kidney, indicating the low dark toxicity, high photo toxicity and excellent bio-compatibility of such NPs.

Introduction

Traditional cancer therapies, such as radiation, surgery and chemotherapy may suffer from invasion, no targeting and inevitably the recurrence of cancer. It is urgent that more therapies should be developed for treatment of cancer. Over the past decades, increasing attention has been attached to photodynamic therapy (PDT), a relatively newly developed one, owing to its non-invasion, low systemic toxicity and etc. [1-11] Among the various factors, the design and preparation of photosensitizer (PS) which can generate reactive oxygen species (ROS) under the irradiation of light plays a significant role in PDT. Common PSs, however, usually tend to form π - π stacking aggregates *via* driving forces such as Vander Waals

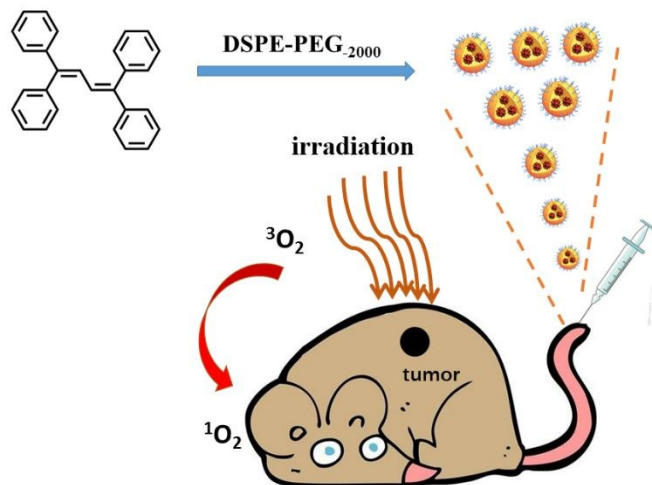
interactions, hydrogen bonding, electrostatic interactions, hydrophobic effects, leading to fluorescence quenching in aqueous solution, which is the so-called aggregation caused quenching (ACQ). Such ACQ effect limits the potential of the PSs as fluorescence imaging agents. Therefore, it is considerably significant to develop PSs that can be both dispersible in aqueous solution and still remain highly fluorescent simultaneously.

Over the past years, great efforts have been spared on the chemical approaches to preventing ACQ [12-26]. Opposite to ACQ, molecules with aggregation induced emission (AIE) property have been synthesized, typically tetraphenylethylene. Such fluorophore have enhanced emission aggregation induced emission (AIE) in that the phenyl rings can undergo active intramolecular rotational/twisting motions alongside the C-C bonds against the stator upon excitation. They can be dissolved in organic solvent while their fluorescence will become stronger in aqueous media, the reason is its self-aggregation driven by limited solubility as well as π - π interactions. [27-28]

- The Third People's Hospital of Kunshan, Kunshan, Jiangsu, 215316, China,
- School of Pharmacy, Guilin Medical University, Guilin 541004, Guangxi, P.R. China. email: zdf1226@126.com
- Department of Chemistry and Materials Engineering, Changshu Institute of Technology, Jiangsu, P.R. China Email: liqiaoyun61@126.com

*Electronic Supplementary Information (ESI) available: [details of any supplementary information available should be included here]. See DOI: 10.1039/x0xx00000x

In our previous work, the anticancer property of (2-(4-bromophenyl)ethene-1,1,2-triyl)tribenzene was investigated both *in vitro* and *in vivo*.^[29] However, the compound has an -Br atom, which will quench the fluorescence of tetraphenylethylene by the spin orbit crossing (SOC). To extend our previous work, 1,1,4,4-tetraphenylbuta-1,3-diene (denoted as **TPD**) have been designed and prepared by self-condensation reaction of 3,3-diphenylacrylaldehyde in the presence of Zn powder and TiCl₄. It is supposed that this compound with strong rigidity can overcome ACQ and shows AIE property. Then 1,2-distearoyl-sn-glycero-3-phospho-ethanolamine-*N*-[methoxy(polyethyleneglycol)-2000] (DSPE-PEG-2000) coated **TPD** can self assemble to form nanoparticles (NPs) which has good dispersity in PBS. To further investigate the cytotoxicity of such NPs, HeLa cells have been selected as the model. MTT assay shows that **TPD** NPs with a low half inhibitory concentration of 8.2 μg/mL are able to induce cell apoptosis upon light irradiation. Furthermore, *in vivo* study show that **TPD** NPs are able to inhibit tumor growth after irradiation at a low dose (0.5 mg/kg) without any side effects towards normal organs, including heart, liver, spleen, lung and kidney, indicating the low dark toxicity, high photo toxicity and outstanding bio-compatibility of such NPs. Our results show that heavy atom free **TPD** with high singlet oxygen generation ability is a potential candidate for cancer therapy both *in vitro* and *in vivo*.



Scheme. Illustration of the **TPD** NPs for photodynamic cancer therapy.

Experimental

Materials and apparatus

All the chemicals were commercially available from sigma and were used without further purification. ¹H NMR and ¹³C NMR spectra were performed on Bruker DRX NMR spectrometer in CDCl₃ at 298 K with solvent residual (CDCl₃, δ = 7.26 ppm) as the internal standard. UV-vis

spectra were measured on a spectrophotometer (UV-3600 UV-Vis-NIR, Shimadzu, Japan). The fluorescence spectra were measured on an F-4600 spectrometer (HITACHI, Japan). DLS was carried out on a 90 Plus particle size analyzer (Brookhaven Instruments, USA). TEM of the nanoparticles were measured on JEOL JEM-2100 equipment.

2.2 Synthesis and characterization of TPD

A mixture of Zn powder (1.12 g, 20 mmol) and 3,3-diphenylacrylaldehyde (2.08 g, 10 mmol) were dissolved in dried THF (100 mL) and the mixture was cooled to -78°C, then N₂ was purged to drive off possible oxygen and water for 2 h. TiCl₄ (2.85g, 15 mmol) was slowly added and the mixture was reacted for another 12 h. The mixture was poured to brine and washed with saturated NaHCO₃ three times (100 mL). Then CH₂Cl₂ was used to extract the crude product three times (100 mL), which was purified by column chromatography on silica gel with CH₂Cl₂/hexane (v/v 1:2) as the eluant. ¹HNMR (300 MHz, CDCl₃) 7.46-7.34 (6H, m), 6.80-6.75 (4H, d), 7.24-7.18 (6H, d), 7.18-7.12 (4H, t); 6.78 (2H, s), ¹³CNMR (125 MHz, CDCl₃) 144.0, 142.5, 140.0, 130.7, 128.2, 128.0, 126.0; Elemental analysis for C₂₈H₂₂: C, 93.81; H, 6.19; found C, 93.86, H, 6.14; MS (ESI) : calcd. m/z = 358.17; found m/z = 358.35.

2.3 Preparation of TPD nanoparticles

The nanoparticles of **TPD** were prepared by nanoprecipitation with DSPE-PEG-2000. DSPE-PEG-5000 (5 mg) was dissolved in distilled water with ultrasound. And then **TPD** (5 mg) was dissolved in tetrahydrofuran (THF, 1 mL). Then 200 μL of such solution was injected into PBS with ultrasound at room temperature. After the mixture was stirred for 10 min, THF was removed by purging nitrogen. The product was then frozen and dried for further use.

2.4 Cell culture and MTT assay

HeLa cell lines were cultured in a regular growth medium consisting of Dulbecco's modified Eagle's medium (DMEM, Gibco) with 10% fetal bovine serum (FBS) and 1% penicillin-streptomycin under an atmosphere of 5% CO₂ at 37 °C. Cell viability assays of the **TPD** NPs were first dissolved in distilled water, which were diluted with DMEM to various concentrations (0-20 μg/mL) and put in the 96-well plate. Then the plate was irradiated with a xenon lamp (30 mW/cm²) for 5 minutes. Cell viability was determined by colorimetric 3-(4,5-dimethylthiazol-2-yl)-2,5-diphenyltetrazolium bromide (MTT) assay. MTT in distilled water (5 mg/mL, 20 μL) was added to each well followed by incubation for 4 h under the same conditions at 37°C. Then the solution was discarded followed by the addition of DMSO (200 μL). At ambient temperature, the

absorbance before 490 nm was measured on a Bio-Tek microplate reader. The cell viability of the control group (without **TPD** NPs) was considered as 100%. The cell viability was then calculated by the following equation: viability (%) = mean absorbance of the group incubated with **TPD** NPs / mean absorbance of the group incubated with DMEM.

2.5 Cellular uptake and fluorescence image of cellular ROS

HeLa cells were incubated with DSPE-PEG-₂₀₀₀ coated **TPD** NPs (8.2 μg/mL, 2 mL) in a confocal dish for different time in dark for 24 h. Then the solution was discarded and the cells were washed with PBS three times (1 mL), followed by the addition of 1 mL polyoxymethylene for 25 min. Then polyoxymethylene was discarded and the cells were washed with PBS for three times (1 mL). The sample with **TPD** NPs for 24 h was further cultured with 10 μM of 2,7-dichlorodihydrofluorescein diacetate (DCF-DA) for another 5 min. Afterwards, it was washed with PBS three times (1 mL). This sample was irradiated by Xenon lamp (30 mW/cm²) for 3 minutes. The fluorescence images were observed by Olympus IX 70 inverted microscope. For the samples with **TPD** NPs for 24 h and they were excited at the wavelength of 433 nm and collected fluorescence from 450 to 600 nm. While the one incubated with DCF-DA under irradiation, it was excited with 488 nm laser and collected fluorescence from 490 to 600 nm.

2.6 In vivo tumor treatment histology examination

The study complies with all institutional and national guidelines, and was approved by the Chinese laws. The protocol was approved by Animal Center of Guilin Medical University (SCXK2007-001). 12 nude mice were purchased and then injected with HeLa cells into the armpit as the tumor source. When the tumor volume reached about 100 mm³, the mice were divided into 3 groups randomly. For the control group, the mice were intravenously injected with saline while the other groups were injected with **TPD** NPs (80 μg/mL, 100 μL) in PBS solution, respectively. After 4 h, the tumors of the irradiation groups were irradiated by Xenon lamp for 10 minutes while the mice in the non-irradiation ones were not irradiated exceptionally. The experiment was continued for twenty eight days, and the tumor volume and body weight of mice were recorded every two days. These nude mice were killed followed by the histology analysis. The main organs (heart, liver, spleen, lung, kidney) and the tumor from each mouse was isolated and fixed in 4% formaldehyde solution. After dehydration, they were embedded in paraffin cassettes and stained with hematoxylin and eosin (H&E), the images were recorded on a microscope.

Results and Discussion

Synthesis and characterization of **TPD** and NPs

The absorbance of **TPD** in THF and the corresponding nanoparticles (NPs) in distilled water were measured. **TPD** in THF show the peak at 247 and 351 nm while the NPs 252 and 345 nm, respectively. However, the absorbance peak of the NPs is broader than that of the **TPD** molecule. Also, the absorbance of NPs in water becomes broader than that in DCM, which may be caused by the aggregation of the NPs in water. In the fluorescence spectra, a large Stokes shift of 105 nm was observed, indicating the potential AIE of such NPs. To further investigate the AIE effect of **TPD** NPs, the fluorescence in THF/water with different fraction was reported. As shown in Figure 1b, with the increasing fraction of water, the fluorescence jump sharply, which is the characteristic of AIE. Transmission electron microscope (TEM) of **TPD** NPs demonstrates that it can self assemble to form nanoparticles with mean diameter of approximate 70 nm, which is consistent with the dynamic light scattering (DLS) results. Since singlet oxygen generation in aqueous solution is essential for PDT, SOSG (singlet oxygen sensor green) was used as a probe. Figure 1d shows the fluorescence enhancement of SOSG with light irradiation. It can be seen that the fluorescence enhancement of **TPD** NPs with irradiation is faster than that of **TPE-Br** NPs, showing the stronger ROS generation ability of **TPD** NPs under irradiation.^[29]

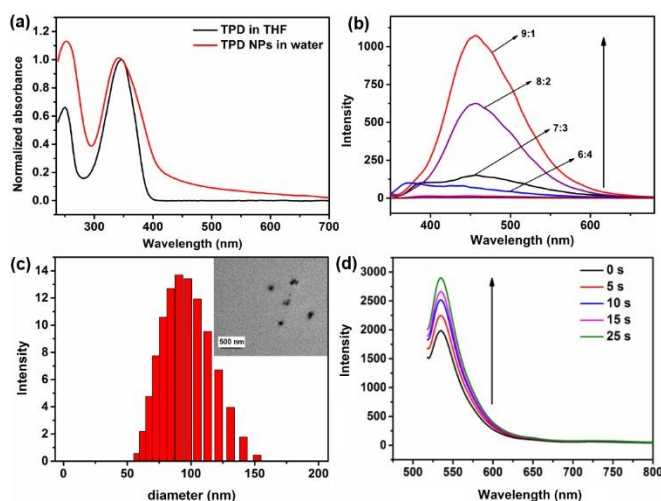


Figure 1 (a) Normalized absorbance of **TPD** in THF and DSPE-PEG-₂₀₀₀ coated **TPD** NPs in water; (b) Fluorescence intensity of **TPD** in THF/water with different fraction (from 1:9 to 9:1); (c) TEM and DLS of DSPE-PEG-₂₀₀₀ coated **TPD** NPs; (d) ROS generation of **TPD** NPs with SOSG as a probe in water.

MTT assay, cellular uptake and ROS generation *in vitro*

To evaluate the suitability of TPD NPs for cell imaging *in vitro*, cellular uptake of DSPE-PEG-₂₀₀₀ coated TPD NPs was recorded using confocal laser scanning microscope (CLSM). TPD NPs could be used as an agent for cell imaging because green fluorescence was observed. 2',7'-dichlorofluorescein diacetate (DCF-DA), the commercial ROS probe, was selected to detect the singlet oxygen generation. It is found that TPD NPs are able to generate singlet oxygen effectively *in vitro* owing to the observed strong green fluorescence upon the excitation at 488 nm (Figure 2b).

To further investigate the phototherapy efficacy of TPD NPs, MTT assay was performed. For one thing, high phototoxicity is fundamental to photodynamic therapy. It can be seen that cell viability has been dramatically suppressed with the increase of the concentration of such NPs, and the half inhibitory concentration (IC_{50}) is as low as 8.2 $\mu\text{g}/\text{mL}$, which is superior to that of TPE-Br NPs (12 $\mu\text{g}/\text{mL}$, TPE-Br = (2-(4-bromophenyl)ethene-1,1,2-triyl)tribenzene)^[29] and ETTDA NPs (40 $\mu\text{g}/\text{mL}$, ETTDA=4,4',4'',4'''-(ethene-1,1,2,2-tetrayl)tetrakis(N,N-diethylaniline))^[30]. For another thing, low dark toxicity is crucial for a photosensitizer to minimize the side effects on normal tissues. The dark toxicity of such NPs is negligible because the cell viability remains high, compared with the control group.

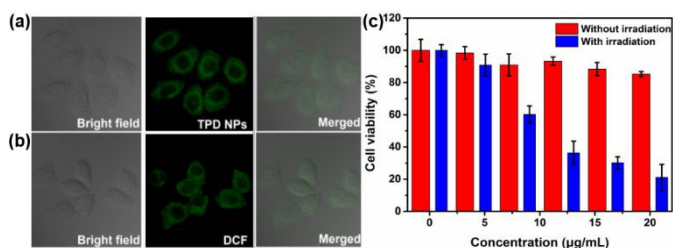


Figure 2 (a) Cellular uptake of TPD NPs in HeLa cells; (b) ROS generation of TPD NPs with DCF-DA as a probe; (c) MTT assay of TPD NPs on HeLa cells with different concentrations (0, 5, 10, 15, 20 $\mu\text{g}/\text{mL}$).

In vivo fluorescence imaging guided photodynamic therapy

Nanoparticles can be passively targeted to the tumor by the enhanced penetration and retention (EPR) effect. Fluorescence imaging has been taken advantage of to investigate the uptake of the NPs in the tumor. As shown in Figure 3a, no detectable fluorescence can be observed when no NPs were injected at 0 h. After 2 h, the

fluorescence of the tumor gradually become stronger while that is the strongest at 6 h injection, demonstrating 6 h is the appropriate for phototherapy. At 24 h, the tumor still remain fluorescent. Then the mouse was sacrificed and the fluorescence intensity of the tumor, heart, liver, spleen and kidney was measured. It can be seen that the fluorescence of the tumor is the strongest, followed by liver and kidney.

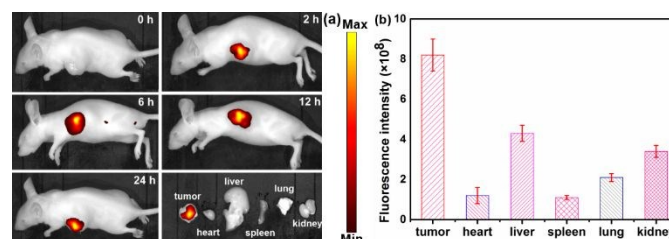


Figure 3 (a) Fluorescence imaging of TPD NPs in HeLa tumor bearing nude mouse at different period of time (0, 2, 6, 12 and 24 h); (b) Fluorescence intensity of tumor, heart, liver, spleen, lung and kidney of the sacrificed mouse after 24 h intravenous injection.

In order to evaluate the phototherapy efficacy of TPD NPs, 12 HeLa tumor-bearing nude mice were divided into three groups at random and used to investigate the PDT efficacy of TPD NPs *in vivo*. As shown in Figure 4a, the relative tumor volume increases quickly while that of the TPD NPs only group a little slowly. The relative tumor volume of the control and the no illumination groups are 12.3 and 11.9, respectively. This can be explained by the fact that irradiation of room light inevitably generate $^1\text{O}_2$ to inhibit the tumor growth. The body weight in the three groups increase, respectively, indicating the low dark toxicity and good bio-compatibility of TPD NPs (Figure 4b). The hematoxylin and eosin (H&E)-stained images of the tumors in the control and TPD NPs only groups (Figure 4g-4i) show the nucleus of HeLa cells remain almost unchanged, suggesting low dark toxicity themselves. In contrast, the nucleus of the irradiation group become distorted or even damaged, indicating the good phototherapy efficacy of TPD NPs. After treatment, these mice were sacrificed and the tumors of the former two groups are put in Figure 4c.

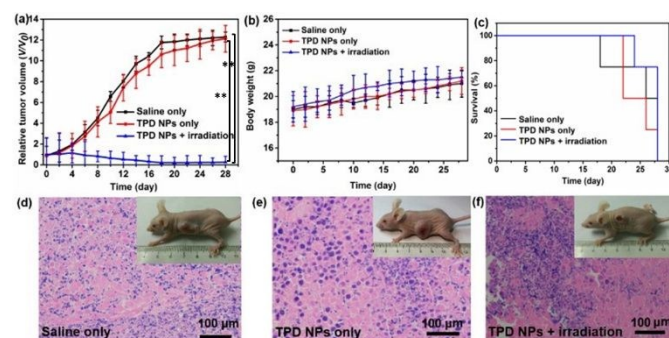


Figure 4 (a) Tumor volume change of the three groups (** $p < 0.01$ compared with control group) (b) Body weight change of the groups; (c) Survival rate of the mice in the control, no irradiation and irradiation groups; (d-f) Photograph and H&E stained pictures of the mice in control, TPD NPs only, TPD NPs + irradiation groups. Scale bar: 100 μm .

To further investigate the bio-compatibility of TPD NPs, the H&E stained pictures of the normal organs have been illustrated in Figure 5. No obvious difference between the images of the main organs (heart, liver, spleen, lung, kidney) in no illumination and illumination groups were observed, indicating TPD NPs cause little damage to normal tissues and the good bio-compatibility of such NPs.^[31-36]

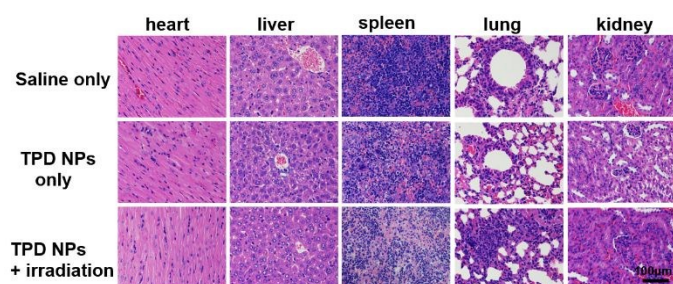


Figure 5 H&E stained picture of the normal organs, including heart, liver, spleen, lung and kidney. Scale bar: 100 μm .

Conclusion

In summary, TPD with aggregation induced emission has been prepared by self Knoevenagel reaction of 3,3-diphenylacrylaldehyde. DSPE-PEG-2000 coated TPD NPs show high fluorescence and singlet oxygen in aqueous solution. *In vitro* study shows that these NPs can be uptaken by HeLa cells and have a low IC_{50} of only 8.2 $\mu\text{g}/\text{mL}$. Furthermore, DSPE-PEG-2000 coated TPD NPs can effectively inhibit the growth of tumors and the normal tissues suffer from no damage, indicating the high phototoxicity, low dark toxicity and good bio-compatibility of such NPs. Other investigation is currently underway in our group.

Acknowledgment

The authors acknowledge financial support from National Natural Science Foundation of China (No. 81460119), the Autonomous Region Level College Students Innovation and Entrepreneurship Training Program (201810601089).

Conflict of interest

The authors have no conflict to declare.

View Article Online
DOI: 10.1039/C9NJ01331H

References

- [1] R.L. Siegel, K.D. Miller, A. J. DVM, *Ca-Cancer J. Clin.* **2018**, *68*, 7-30.
- [2] W.P. Fan, P. Huang, X.Y. Chen, *Chem. Soc. Rev.*, **2016**, *45*, 6488-6519.
- [3] Z.J. Zhou, J.B. Song, L.M. Nie, X.Y. Chen, *Chem. Soc. Rev.*, **2016**, *45*, 6597-6626
- [4] Y.J. Liu, P. Bhattarai, Z.F. Dai, X.Y. Chen, *Chem. Soc. Rev.* **2018**, DOI: 10.1039/c8cs00618k
- [5] M. Laine, N.A. Barbosa, A. Kochel, B. Osiecka, G. Szewczyk, T. Sarna, P. Ziólkowski, R. Wieczorek, and A. Filarowski, *Sensors and Actuators B: Chemical.*, **2017**, *238*, 548-555.
- [6] A. Kamkaew, S. H. Lim, H. B. Lee, L. V. Kiew, L. Y. Chung, K. Burgess. *Chem. Soc. Rev.* **2013**, *42*, 77-88.
- [7] M. Li, Y. Gao, Y. Y. Yuan, Y. Z. Wu, Z. F. Song, B. Z. Tang, B. Liu, Q. C. Zheng, *ACS Nano* **2017**, *11*, 3922-3932.
- [8] X. L. Cai, C. J. Zhang, F. T. W. Lim, S. J. Chan, A. Bandla, C. K. Chuan, F. Hu, S. D. Xu, N. V. Thakor, L. D. Liao, B. Liu, *Small* **2016**, *12*, 6576-6585.
- [9] C. A. Hunter, M. K. J. Sanders, *Photochem. Photobiol.*, **2013**, *88*, 1011-1019.
- [10] C. A. Hunter, J. K. M. Sanders, *J. Am. Chem. Soc.*, **1990**, *112*, 5525-5534.
- [11] U. Siggel, U. Bindig, C. Endisch, T. Komatsu, E. Tsuchida, E. Voigt, J.H. Fuhrhop, Ber. Bunsenges. *Phys. Chem.*, **1996**, *100*, 2070-2075.
- [12] A.T. Han, H.M. Wang, R.T. K. Kwok, S.L. Ji, J. Li, D.L. Kong, B.Z. Tang, B. Liu, Z.M. Yang, D. Ding, *Anal. Chem.* **2016**, *88*, 3872-3878
- [13] M. Li, Y. Gao, Y. Y. Yuan, Y. Z. Wu, Z. F. Song, B. Z. Tang, B. Liu, Q. C. Zheng, *ACS Nano*, **2017**, *11*, 3922-3932
- [14] Y. Y. Yuan, C. J. Zhang, M. Gao, R. Y. Zhang, B. Z. Tang, B. Liu, *Angew. Chem. Int. Ed.* **2015**, *54*, 1780-1786
- [15] Y. Y. Yuan, C. J. Zhang, S. D. Xu, B. Liu, *Chem. Sci.*, **2016**, *7*, 1862-1866
- [16] G. X. Feng, R. T. K. Kwok, B. Z. Tang, B. Liu, *Applied Phys. Rev.* **2017**, *4*, 021307;

- [17] E. Sen, K. Meral, S. Atilgan, *Chem. Eur. J.* **2016**, *22*, 736-745;
- [18] E.J. Wang, E.G. Zhao, Y.N. Hong, J.W.Y. Lam, B.Z. Tang, *J. Mater. Chem. B*, **2014**, *2*, 2013-2019
- [19] Z.Y. Fan, D.D. Li, X. Yu, Y.P. Zhang, Y. Cai, J.J. Jin, J.H. Yu, *Chem. Eur. J.* **2016**, *22*, 3681-3685.
- [20] S.D. Xu, Y.Y. Yuan, X.L. Cai, C.J. Zhang, F. Hu, J. Liang, G.X. Zhang, D.Q. Zhang, B. Liu, *Chem. Sci.*, **2015**, *6*, 5824-5830
- [21] Z.F. Chang, L.M. Jing, B. Chen, M.S. Zhang, X.L. Cai, J.J. Liu, Y.C. Ye, X.D. Lou, Z.J. Zhao, B. Liu, J.L. Wang, B.Z. Tang, *Chem. Sci.*, **2016**, *7*, 4527-4536.
- [22] Y.Y. Yuan, C.J. Zhang, R.T.K. Kwok, D. Mao, B.Z. Tang, B. Liu, *Chem. Sci.*, **2017**, *8*, 2723-2728
- [23] X.Y. Gao, G.X. Feng, P. N. Manghnani, F. Hu, N. Jiang, J.Z. Liu, B. Liu, J.Z. Sun, B.Z. Tang, *Chem. Commun.*, **2017**, *53*, 1653-1656
- [24] B.B. Gu, W.B. Wu, G.X. Xu, G.X. Feng, F. Yin, P.H. Joo Chong, J.L. Qu, K.T. Yong, B. Liu, *Adv. Mater.* **2017**, *1701076*
- [25] X.L. Cai, C.J. Zhang, F. T. Wei Lim, S.J. Chan, A. Bandla, C.K. Chuan, F. Hu, S.D. Xu, N.V. Thakor, L.D. Liao, B. Liu, *Small* **2016**, *12*, 6576-6585
- [26] C.J. Zhang, G.X. Feng, S.D. Xu, Z.S. Zhu, X.M. Lu, J.Wu, B. Liu, *Angew. Chem. Int. Ed.* **2016**, *55*, 6192 -6196
- [27] M. Yamaguchi, Sh. Ito, A. Hirose, K. Tanaka, Y. Chujo, *Mater. Chem. Front.* **2017**, *1*, 1573-157,
- [28] W. Zheng, G. Yang, S.T. Jiang, N.N. Shao, G.Q. Yin, L. Xu, X.P. Li, G.S. Chen, H.B. Yang, *Mater. Chem. Front.* **2017**, *1*, 1823-1828
- [29] J. Yang, X.Q. Gu, W.T. Su, X.Y. Hao, Y.J. Shi, L.Y. Zhao, D.F. Zou, G.W. Yang, Q.Y. Li, J.H. Zou, *Mater. Chem. Front.*, **2018**, *2*, 1842-1846.
- [30] Q.Y. Li, Z.Y. Yang, W.T. Su, D.Y. Chen, G.W. Yang, D. F. Zou, *Chem Select* **2018**, *3*, 2332 -2335.
- [31] L. Huang, Z. J. Li, Y. Zhao, J. Y. Yang, Y. C. Yang, A. J. Pendharkar, Y. W. Zhang, S. Kelmar, L.Y. Chen, W. T. Wu, J. Z. Zhao, G. Han., *Adv. Mater.* **2017**, *29*, 1604789.
- [32] H. He, S. S. Ji, Y. He, A. J. Zhu, Y. L. Zou, Y. B. Deng, H. T. Ke, H. Yang, Y. L. Zhao, Z. Q. Guo, H. B. Chen., *Adv. Mater.* **2017**, *29*, 1606690.
- [33] Z. Yang, R. Tian, J. Wu, Q.L. Fan, B.C. Yung, G. Niu, O. Jacobson, Z.T. Wang, G. Liu, G. Yu, W. Huang, J.B. Song, X.Y. Chen, *ACS Nano*, **2017**, *11*, 4247-4255.
- [34] Z. Yang, Y.L. Dai, C. Yin, Q.L. Fan, W. Zhang, J.B. Song, G.C. Yu, W. Tang, W.P. Fan, B. C. Yung, J. Li, X. Li, X. Li, Y. Tang, W. Huang, J.B. Song, X.Y. Chen, *Adv. Mater.*, **2018**, *30*, 1707509.
- [35] Z. Yang, J.B. Song, W. Tang, W.P. Fan, Y.L. Dai, Z.Y. Shen, L.S. Lin, S. Cheng, Y. Liu, G. Niu, P. Rong, W. Wang, X.Y. Chen, *Theranostics*, **2019**, *9*, 526.
- [36] Z. Yang, Y.L. Dai, L. Shan, Z.Y. Shen, Z.T. Wang, B.C. Yung, O. Jacobson, Y. Liu, W. Tang, S. Wang, L.S. Lin, G. Niu, P. Huang, X.Y. Chen, *Nanoscale Horiz.*, **2019**, *4*, 426-433